Seasonal stratification regulates carbon allocation between particulate and dissolved pathways in the Gulf of Aqaba

Eyal Rahav[1,2,3*] and Adina Paytan[2]

[1] Israel Oceanographic and Limnological Research, Haifa, Israel.
[2] Institute of Marine Science, University of California, Santa Cruz, CA, USA.
[3] Department of Earth and Environmental Science, Ben-Gurion University of the Negev, Beer Sheva, Israel.

*Corresponding author: eyrahav@ucsc.edu; eyal.rahav@ocean.org.il

Abstract

Water column stratification exerts fundamental control on microbial carbon cycling in oligotrophic areas of the ocean, yet its impact on the partitioning and fate of newly fixed carbon remains insufficiently resolved. Here, we investigated carbon fluxes in the Northern Red Sea (Gulf of Aqaba) from 5 cruises conducted during the stratified period. We report ^{14}C-based measurements of primary production partitioned into particulate (>0.7 µm; PP_{POC}) and dissolved (<0.7 µm; PP_{DOC}) fractions, bacterial production (BP), community and bacterial respiration (BR) across the euphotic zone. As stratification intensifies and nutrient supply from depth diminishes, depth-integrated PP_{POC} declined from 1.26 to 0.35 g C m^{-2} d^{-1} while the relative contribution of dissolved carbon pathways increases. The fraction of newly fixed carbon released as dissolved organic carbon (extracellular release; PER) increased from 2.5% to >7% of total PP, indicating that a larger fraction of photosynthetically fixed carbon was released into the dissolved C pool. PP_{DOC} (0.02-0.03 g C m^{-2} d^{-1}) was positively correlated with BP (0.08-0.16 g C m^{-2} d^{-1}), suggesting that recently released dissolved substrates contribute to sustaining heterotrophic microbial activity. Despite declining primary production, BR remained substantial (0.23-0.52 g C m^{-2} d^{-1}), resulting in low to moderate bacterial growth efficiency (13-35%) and indicating that most processed carbon was respired rather than incorporated into biomass. These findings indicate that summer stratification enhances the relative importance of dissolved carbon release and microbial recycling of DOC, thereby reducing the efficiency of carbon transfer to depth in the Gulf of Aqaba and likely other oligotrophic systems.

Key words

Microbial carbon cycling; Oligotrophic seas; Primary production; Bacterial growth efficiency (BGE); Extracellular carbon release (PER).

1. Introduction

Much of the open ocean is characterized by chronic oligotrophy, which shapes the pathways and efficiency of carbon transformation in surface waters (Marañón et al., 2003; Polovina et al., 2008). Under such nutrient-depleted conditions, primary production (PP) tends to be low/negligible and is predominantly supported by small-celled phytoplankton that can cope persistent resource limitation (Dore et al., 2008; Pennington et al., 2006; Reich et al., 2022). Under such conditions, newly fixed carbon is largely retained and remineralized within the microbial loop, where strong coupling between phytoplankton and bacteria controls its subsequent fate (Azam and Malfatti, 2007; Zhang et al., 2025). As a result, the transfer efficiency of carbon to higher trophic levels or its export to depth is often low (Armengol et al., 2019; Alkalay et al., 2020; Roshan and DeVries, 2017; Torfstein et al., 2020).

The onset and relaxation of stratification largely determine how nutrients are delivered to surface waters and thus govern microbial dynamics in oligotrophic environments (Dave and Lozier, 2010; Reich et al., 2026; Signorini et al., 2015). With strengthening stratification, the exchange between deep, nutrient-rich waters and the surface diminishes, causing nutrients in the euphotic zone to become progressively depleted (Chen et al., 2021; Hazan et al., 2018; Lozier et al., 2011). This imposes strong physiological constraints on phytoplankton growth and activity due to limited nutrient availability (Rahav et al., 2016; Zohary et al., 2005). Under these conditions, a considerable portion of newly produced organic carbon can be exuded by phytoplankton as dissolved organic matter (DOC) via extracellular release (Kang et al., 2022; Morana et al., 2014; Thornton, 2014). The resulting DOC provides a substrate for heterotrophic bacteria and forms an important conduit between autotrophic production and heterotrophic metabolism. This recently fixed DOC can be reused and account for a substantial proportion of total carbon fixation under nutrient-limited conditions (abovementioned references).

The fate of DOC in the ocean is largely determined by heterotrophic bacteria, whose metabolic activity often controls whether carbon is retained within the euphotic layer or transferred as particulate organic carbon (POC) to depth (Baetge et al., 2021; LaBrie et al., 2022; Mentges et al., 2019). Bacterial carbon uptake and respiration together define the efficiency of bacterial organic carbon utilization, typically expressed as bacterial growth efficiency, BGE (del Giorgio and Cole, 1998). Oligotrophic waters commonly exhibit low BGE, indicating that much of the assimilated carbon is respired rather than incorporated into cellular biomass (Alothman et al., 2025; Anderson and Turley, 2003; del Giorgio et al., 1997). Such conditions promote fast and efficient carbon cycling within the surface ocean and further

bias the system toward recycling rather than export (del Giorgio and Cole, 1998). The relative magnitudes of PP and community respiration (CR) therefore serve as a useful indicator of the system's metabolic status and offers insight into whether the system is characterized by net carbon accumulation or rapid remineralization (Izett et al., 2024; Stanley et al., 2010).

The Gulf of Aqaba (northern Red Sea) is an oligotrophic basin whose physical and biogeochemical properties are highly affected by seasonal and interannual variability (Laiolo et al., 2014; Rahav et al., 2015; Reich et al., 2024). During winter, deep convective mixing injects nutrients into the surface layer, often leading to increased phytoplankton biomass and productivity (Lindell and Post, 1995; Avrahami et al., 2025). Differently, in summer, a strongly stratified water column results in severe nutrient depletion (Meder et al., 2012) and subsequently low phytoplankton biomass and activity (Lindell and Post, 1995; Reich et al., 2024). Despite extensive characterization of the physical and chemical seasonal cycles in the Gulf of Aqaba (Biton and Gildor, 2011), and the recognized dominance of microbial recycling in oligotrophic waters (e.g., low *f-ratios*, Alothman et al., 2025), the corresponding shifts in microbial carbon processing, particularly the partitioning of the carbon fixed during the stratified season between particulate matter, dissolved carbon released from cells, and heterotrophic utilization of this carbon, remain insufficiently resolved.

Here, we investigate microbial carbon cycling during the summer stratified period in the Gulf of Aqaba, focusing on how progressive nutrient depletion influences the balance between carbon fixation, release, and remineralization. To this end, we combined measurements of primary production, dissolved organic carbon release, and heterotrophic bacterial activity from 5 monthly cruises, to assess how the structure and efficiency of carbon processing evolve over the course of the stratified season.

2. Material and methods

2.1. Study site

Seawater was collected across the euphotic zone (0-100 m) at 20 m depth intervals at an offshore station in the northern Gulf of Aqaba, Red Sea (29.47°N, 34.92°E). Sampling was conducted monthly from May to September 2023, spanning the transition from late spring to late summer. Measurements included a comprehensive set of microbial activity measurements, including particulate primary productivity (>0.7 µm PP_{TOT}), dissolved primary production (PP_{DOC}, <0.7 µm), bacterial production (BP), and community respiration (CR). Ancillary data

comprised Conductivity, Temperature, Depth (CTD) and photosynthetically active radiation (PAR) profiles (Sea-Bird SBE 19plus), inorganic nutrients concentration, and chlorophyll *a* measurement.

2.2. Particulate and dissolved primary production and extracellular release

Autotrophic activity was assessed by measuring particulate primary productivity (PP_{POC}) and carbon fixed present in the dissolved fraction (PP_{DOC}), enabling a detailed partitioning of carbon flow pathways within the microbial food web. To this end, seawater was collected in triplicate 50 ml acid-washed Falcon tubes. The collected samples were spiked with $NaH^{14}CO_3$ (Perkin Elmer, specific activity 56 mCi $mmol^{-1}$) at a final radioisotope dilution of $1:10^4$ *v:v* (1 µCi/10 ml) and incubated for 24 h under ambient temperature and light. Incubations were stopped by filtration of the ^{14}C-enriched water samples through glass fiber filters (GF/Fs) (0.7 µm nominal pore size, PP_{POC}) using low vacuum pressure (<50 mmHg). Filtration was performed under gentle vacuum pressure to minimize cell disruption, intracellular carbon release, and cell breakthrough. Although GF/F filters have a nominal pore size of ~0.7 µm, their depth-filtration properties allow efficient retention of small picocyanobacterial (e.g., *Prochlorococcus*) under low-pressure filtration conditions (Bertilsson et al., 2003). Filtrate samples (5-10 ml, PP_{DOC}) were also collected in 15 ml Faclon tubes. Filters were rinsed with 5 ml of sterile-filtered seawater collected from the same site (<0.22 µm) and the samples were subsequently acidified with 50 µl of 37% hydrochloric acid (HCl, lowering pH to <2) and left open in a fume hood overnight to allow conversion of all DIC to carbon dioxide (CO_2) and complete degassing and removal of inorganic carbon as $^{14}CO_2$. Filters were transferred into glass vials and 5 ml of scintillation cocktail (Ultima Gold) was added. To determine PP_{DOC}, the filtrate (10 ml) was transferred to scintillation vials, acidified with 50 µl hydrochloric acid and 5ml scintillation cocktail was added as above (Teira et al., 2001). Samples were counted using a TRI-CARB 4810 TR (Packard) liquid scintillation counter. Blank samples (for both PP_{POC} and PP_{DOC}) collected from each depth were spiked with $NaH^{14}CO_3$ and filtered immediately without incubation. These blanks yielded negligible counts, and their reads were subtracted from their respective samples read. Added activity of the radiolabeled 'working solution' was obtained in each campaign by removing 50 µl from random samples immediately after spiking and before incubation (usually one per sampling depth), placing it on a new GF/F filter, adding 50 µl ethanolamine and scintillation liquid, and counting immediately. The variability between the 'added activity' measurements was usually negligible for the same work solution (prepared

freshly before each campaign), and we therefore used the average value of all collected samples/depths on each cruise.

PP_{POC} and PP_{DOC} rates were calculated based on the Bermuda Atlantic Time-series Study (BATS) protocol (https://www.bco-dmo.org/dataset/893182/description#acquisition) using the equation:

$$(1)\ \text{Primary productivity} = \frac{(\text{DPM} - \text{blank})}{\text{V}} \times \text{DIC} \times \frac{\text{AA vol}}{\text{TDPM}} \times \text{f} \times \frac{1}{\text{t}}$$

DPM equals the disintegrations per minute, V = the filtered volume, DIC is the dissolved inorganic carbon in seawater calculated from total alkalinity; ~25 µg C L^{-1}), AA vol = Added activity volume, TDPM = Total ^{14}C disintegration per minute, t = incubation time, and f = factor correcting the uneven uptake of ^{14}C due to fractionation (1.05).

The percentage of extracellular release (PER; %) was calculated as follows:

$$(2)\ \text{PER}\ (\%) = \frac{\text{PP\_DOC}}{\text{PP\_POC+PP\_DOC}} \text{x}\ 100$$

2.3. Bacterial productivity (BP)

Triplicate seawater samples (1.7 ml) from each sampling depth were incubated in the dark under ambient temperature with 10 nmol L^{-1} of ^{3}H-leucine (Perkin Elmer; specific activity 123 Ci $mmol^{-1}$) for 4 h, at *in situ* temperature, following the protocol of Simon et al., (1990). Incubations were terminated by the addition of 100 µl of 100% trichloroacetic acid (TCA), and samples were subsequently processed using the microcentrifugation method (Smith and Azam, 1992). After processing, 1 ml of scintillation cocktail (Ultima Gold) was added to each vial, and radioactivity was measured using a TRI-CARB 4810 TR (Packard) liquid scintillation counter. Random 'killed' controls, containing ^{3}H-leucine and TCA added prior to incubation were used to account for background activity. Leucine incorporation rates were converted to carbon production using a conversion factor of 3 kg C mol^{-1} leucine, assuming an isotopic dilution factor of 2 (Simon and Azam, 1989).

2.4. Community and bacterial respiration

Community respiration (CR) rates were estimated from dark triplicate incubations per depth under ambient temperature. Dissolved O_2 concentrations were measured using an optical oxygen meter (FireSting, PyroScience GmbH) equipped with fiber-optic sensors. Prior to the incubations, optical sensor spots (OXSP5, PyroScience) were affixed to the inner wall of Winkler bottles (300 ml) according to the manufacturer's instructions. Bottles were carefully

filled to avoid bubble formation and sealed with ground-glass stoppers. Samples were incubated for 24 h under continuous, gentle stirring using magnetic stir bars to ensure homogeneous O_2 distribution without introducing air bubbles or disturbing the sensor spot. The system was calibrated prior to measurements using a two-point calibration (air-saturated seawater and zero-oxygen solution) following the manufacturer's guidelines. CR was calculated as the temporal change in O_2 concentration (T_{24} minus T_0) normalized to the incubation duration (Cheung et al., 2024). The detection limit was 0.5 µmol O_2 L^{-1}. CR was converted into BR using the linear regression of Aranguren-Gassis et al., (2012):

$$(3)\ BR = 0.3xCR^{1.22} - 0.013$$

A respiratory quotient of 1 was used to convert O_2 consumption into carbon respiration (del Giorgio and Cole, 1998). Bacterial growth efficiency (BGE) was calculated as follows (del Giorgio and Cole, 1998):

$$(4)BGE\ (\%) = \frac{BP}{BP + BR} x\ 100$$

2.5. Inorganic nutrients

Samples were collected in acid-washed plastic Falcon tubes without prefiltration and kept frozen at -20 °C until analysis within a few months. One sample per depth was collected. Nitrate+nitrite (NO_2+NO_3), orthophosphate (PO_4) and silicic acid ($Si(OH)_4$) were measured with a Seal Analytical AA-3 system (Kress and Herut, 2001). The limits of detection (twice the standard deviation of the blank) were 0.03 µM for nitrate+ nitrite, 0.008 µM for orthophosphate, and 0.05 µM for silicic acid. Ammonium (NH_4) concentrations were measured fluorometrically using the orthophthaldialdehyde (OPA) method (Holms et al., 1999) using a Turner Designs (Trilogy) fluorometer equipped with 365-nm excitation and 460-nm emission filters. The detection limit was 0.01 µM. The quality of the nutrient measurements is regularly confirmed by inter-comparison exercises (e.g., QUASIMEME program).

2.6. Chlorophyll a

Seawater (300 ml) samples were filtered through GF/F and stored at -20 °C in a dark box. One sample per depth was collected. Samples were extracted overnight in 5 ml of 90% acetone at 4 °C in the dark (Welschmeyer, 1994). Chlorophyll concentrations were determined using a Turner Designs (Trilogy) fluorometer with 436-nm excitation and 680-nm emission filters.

2.7. Statistical analyses

Pairwise relationships among environmental and biological variables were assessed using Pearson correlation analysis. All data points from the upper 0–100 m across the five sampling campaigns were included. Prior to analysis, data were screened for missing values, and only complete datasets were retained. Pearson correlation coefficients (r) and corresponding p-values were calculated to assess the strength and significance of pairwise relationships. Statistical significance was evaluated at two levels ($p<0.05$ and $p<0.01$). Correlation matrices were visualized using a lower-triangle format to improve readability, with color gradients representing correlation strength and overlaid values indicating correlation coefficients and their significance levels. Analyses and figure generation were performed using Python (version 3.13).

3. Results

The surface water (0-20 m) was consistently warm throughout the study period (25-28 °C) and showed a clear seasonal increase in temperature from early to mid-summer (Figure 1A). The mixed layer depth (MLD), estimated from a temperature threshold criterion (ΔT = 0.2 °C from surface values, de Boyer Montégut et al., 2004), shoaled progressively from 45 m in early summer (May) to 15-20 m during peak stratification (July-August), before slightly deepening again in September (28 m). A pronounced vertical temperature gradient was evident throughout the sampling period, with temperatures decreasing to 23-24 °C at 100 m (Figure 1A). Inorganic nutrient concentrations were generally low throughout the upper water column and increased with depth across the 0-100 m layer (Figure 1B-D). Photosynthetically active radiation (PAR) ranged from 1200-1950 μmol quanta m^{-2} s^{-1} at the surface and declined exponentially with depth, reaching <20 μmol quanta m^{-2} s^{-1} at 100 m, equivalent to 0.5-1.8% of surface irradiance (Table 1). Nitrate+nitrite (NO_3+NO_2) concentration ranged from below detection level (<0.03 μmol L^{-1}) to 0.14 μmol L^{-1} (Figure 1B), resulting in integrated values of 4.5-11.2 μmol m^{-2} (Table 1). NO_3+NO_2 concentrations were only slightly higher below the MLD (Figure 1B), indicating restricted nutrient supply from the nutricline to the upper euphotic zone during summertime. The sporadic elevated NOx concentrations (e.g., 20 m in June and 40 m in August, Figure 1B) likely represent outlying measurements associated with the analysis of unfiltered and freezed samples (Krom et al., 2005; Reed et al., 2023). Similar sporadic NOx peaks were previously reported in the Gulf of Aqaba using similar methodology (Meeder et al., 2012; Rahav et al., 2026; Reich et al., 2024). Importantly, these values have a negligible effect on the depth-integrated NOx inventories (Table 1) and do not alter the broader seasonal

patterns. Ammonium (NH_4) concentrations were also low, ranging from 12 to 65 nmol L^{-1}, and increased with depth (Figure 1C). Depth-integrated NH_4 concentrations were higher during mid- to late summer (3.0-4.6 µmol m^{-2}) compared to early summer (1.7 µmol m^{-2}; Table 1). Orthophosphate (PO_4) was usually low throughout the water column and across all sampling periods; 0.01-0.03 µmol L^{-1}, except for a single elevated surface value of 0.07 µmol L^{-1} observed during the September cruise (Figure 1D). The integrated PO_4 was low and ranged from 2.1-4.3 µmol m^{-2} (Table 1). The resulting N:P ratio was below the canonical Redfield ratio of 16:1 (Redfield, 1934) and ranged from 1.8:1 to 7.5:1 (Table 1), suggesting N limiting conditions for the microbial populations (Tanioka et al., 2022). Silicic acid ($Si(OH)_4$) concentrations were relatively homogeneous throughout the water column (Figure 1E). However, higher levels were observed in May-June (1 µmol L^{-1}, 75-89 µmol m^{-2}), followed by a decline during July-September (<0.6 µmol L^{-1}, 55 µmol m^{-2}) (Figure 1E, Table 1), suggesting a transition from a diatom-influenced system in spring/early summer to an oligotrophic, small-cell-dominated community under more stratified conditions (Avrahami et al., 2025).

Chlorophyll *a* exhibited a pronounced vertical structure across all sampling periods (Figure 2A). Surface concentrations were typically low, ranging from 0.05 to 0.15 µg L^{-1}, and increased with depth to form a well-defined deep chlorophyll maximum (DCM). The DCM was consistently located between 60 and 100 m, coinciding with the lower euphotic zone. Chlorophyll concentrations at the DCM ranged from 0.3 to 0.7 µg L^{-1}, representing a several-fold increase relative to surface waters. Vertically integrated chlorophyll biomass (0-100 m) ranged from 16 to 28 mg m^{-2} across the study period (Table 1). Integrated biomass was lowest in early summer (May-June; 16-20 mg m^{-2}) and increased toward mid/late-summer (July-September; 25-28 mg m^{-2}).

Particulate primary production (PP_{POC}) exhibited a pronounced vertical gradient across all sampling periods, with highest rates observed in surface waters and a progressive decline with depth (Figure 2B). Surface PP_{POC} ranged from 25 µg C L^{-1} d^{-1} in early summer and decreased to 8 µg C L^{-1} d^{-1} during mid- to late summer (Figure 2B). Below 40-60 m, PP_{POC} declined substantially in all stations and ranged from 8 µg C L^{-1} d^{-1} in May to 1 µg C L^{-1} d^{-1} in June-September (Figure 2B). Depth-integrated PP_{POC} ranged from 0.28 to 1.26 g C m^{-2} d^{-1} (Table 1), with the highest PP_{POC} values observed in early summer (May), followed by a marked decline toward mid-summer (June-August), and a slight increase in September. This seasonal decrease in integrated PP_{POC} coincided with the progressive shoaling of the mixed layer (Table 1, Figure 1A) and reduced nutrient availability in surface waters (Figure 1B-E),

and is in agreement with previous observations in the Gulf of Aqaba (Iluz et al., 2009; Reich et al., 2024). PP_{DOC} generally displayed its highest rates in the upper water column (Figure 2C). In June-September, PP_{DOC} was elevated in surface and near-surface waters, typically ranging from 0.2 to 0.5 µg C L^{-1} d^{-1}, and then declined progressively with depth. Below 80 m, rates were consistently lower than 0.10 µg C L^{-1} d^{-1}. In contrast, the May profile was uniform throughout the water column (0.4 µg C L^{-1} d^{-1}). Despite these differences in vertical distribution, depth-integrated PP_{DOC} varied only slightly across months, ranging from 0.02 to 0.03 g C m^{-2} d^{-1} (Table 1). The percentage of extracellular organic carbon release (PER) increased over the course of the summer and showed a clear depth dependence (Figure 2D). In May, PER was generally low and relatively uniform (<5%), consistent with the homogeneous distribution of PP_{DOC} (Figure 2C). In contrast, from June onward PER was lower in the upper water column (<10%) and increased with depth, with the highest values typically observed below 40-60 m, near the base of the euphotic zone reaching as high as 20%. Integrated PER rose from 2.5% in May to 5.7-6.4% during June-August and reached 7.4% in September (Table 1).

Heterotrophic prokaryotic (bacterial) production (BP) exhibited moderate vertical and temporal variability (Figure 3A). BP rates were generally highest in the upper water column (0-40 m), ranging from 0.8 to 2.5 µg C L^{-1} d^{-1}, and declined with depth. Below 60-80 m, BP decreased substantially, with values commonly <1 µg C L^{-1} d^{-1} near the base of the euphotic zone. Depth-integrated BP ranged from 0.08 to 0.16 g C m^{-2} d^{-1} across the study period, with the higher values observed during mid- to late summer (Table 1). BR was high and relatively homogeneous throughout the water column in May-June, with rates typically around 4-8 µg C L^{-1} d^{-1} (Figure 3B), summing to 0.4-0.5 g C m^{-2} d^{-1} over the upper 100 m (Table 1). Differently, during July-August, BR exhibited a stronger vertical variability with higher respiration rates recorded in the upper 40-60 m (4-5 µg C L^{-1} d^{-1}) and lower at the bottom of the euphotic layer around 0-40 m (1-2 µg C L^{-1} d^{-1}). In September, BR again showed relatively low vertical variability, with rates mostly between 1 and 4 µg C L^{-1} d^{-1}, corresponding to 0.25 g C m^{-2} d^{-1}.

The spatial and vertical distribution of bacterial growth efficiency (BGE, Figure 3C) broadly mirrored that of BR (Figure 3B) and was consistent with patterns observed for BP (Figure 3A). In all months, relatively higher BGE values were found in the upper 0-60 m, whereas lower values were typically observed at greater depths (Figure 3C). Temporally, BGE was lower during May-June, when values throughout the water column were typically 10-20% (integrated value 13%, Table 1), reflecting the relatively high and vertically homogeneous BR

during this period (Figure 3C). In contrast, from July onward, BGE increased in the upper water column, commonly reaching 20-40% in the 0-60 m layer and 10-20% below 60 m (Figure 3C), summing 28-30% over the whole euphotic layer (Table 1). In September, BGE exhibited reduced vertical variability, with values generally ranging between 15 and 30% across the water column (Figure 3C).

Pearson correlation analysis revealed that depth and temperature were the dominant structuring variables, with depth negatively correlated with temperature ($r=-0.83$, $p<0.01$) and strongly positively correlated with chlorophyll *a* ($r=0.89$, $p<0.01$), reflecting the vertical separation between surface waters and the DCM (Figure 4). Depth was also negatively correlated with both PP_{POC} ($r=-0.54$, $p<0.01$) and PP_{DOC} ($r=-0.63$, $p<0.01$) (Figure 4), indicating that autotrophic activity was mainly concentrated in the upper euphotic zone (Figure 2B, C). As expected, PP_{POC} positively correlated with PP_{DOC} ($r=0.69$, $p<0.01$) (Figure 4), demonstrating that the release of dissolved organic carbon scales with total photosynthetic activity. At the same time, PP_{POC} showed a significant negative correlation with chlorophyll *a* ($r=-0.46$, $p<0.05$) (Figure 4), suggesting a decoupling between biomass accumulation and photosynthetic rates as found for chlorophyll *a* (Figure 2). Interestingly, PP_{DOC} exhibited several key relationships that highlight its central role in carbon cycling in the Gulf of Aqaba during summertime. For example, PP_{DOC} was positively correlated with PO_4 ($r=0.47$, $p<0.05$), and negatively correlated with chlorophyll *a* ($r=-0.58$, $p<0.01$) (Figure 4). These patterns indicate that PO_4 may be preferentially regenerated from following the DOC released from the cells. Furthermore, PP_{DOC} was positively correlated with BP ($r=0.50$, $p<0.01$) (Figure 4), supporting the role of PP_{DOC} as an important substrate fueling heterotrophic activity in the Gulf of Aqaba. In contrast, inorganic nitrogen species (e.g., NO_3+NO_2, NH_4) showed weak or non-significant relationships with PP_{POC} or PP_{DOC} (Figure 4), suggesting these N species are utilized as fast as they released from cells or that they are not released as much as carbon and orthophosphate.

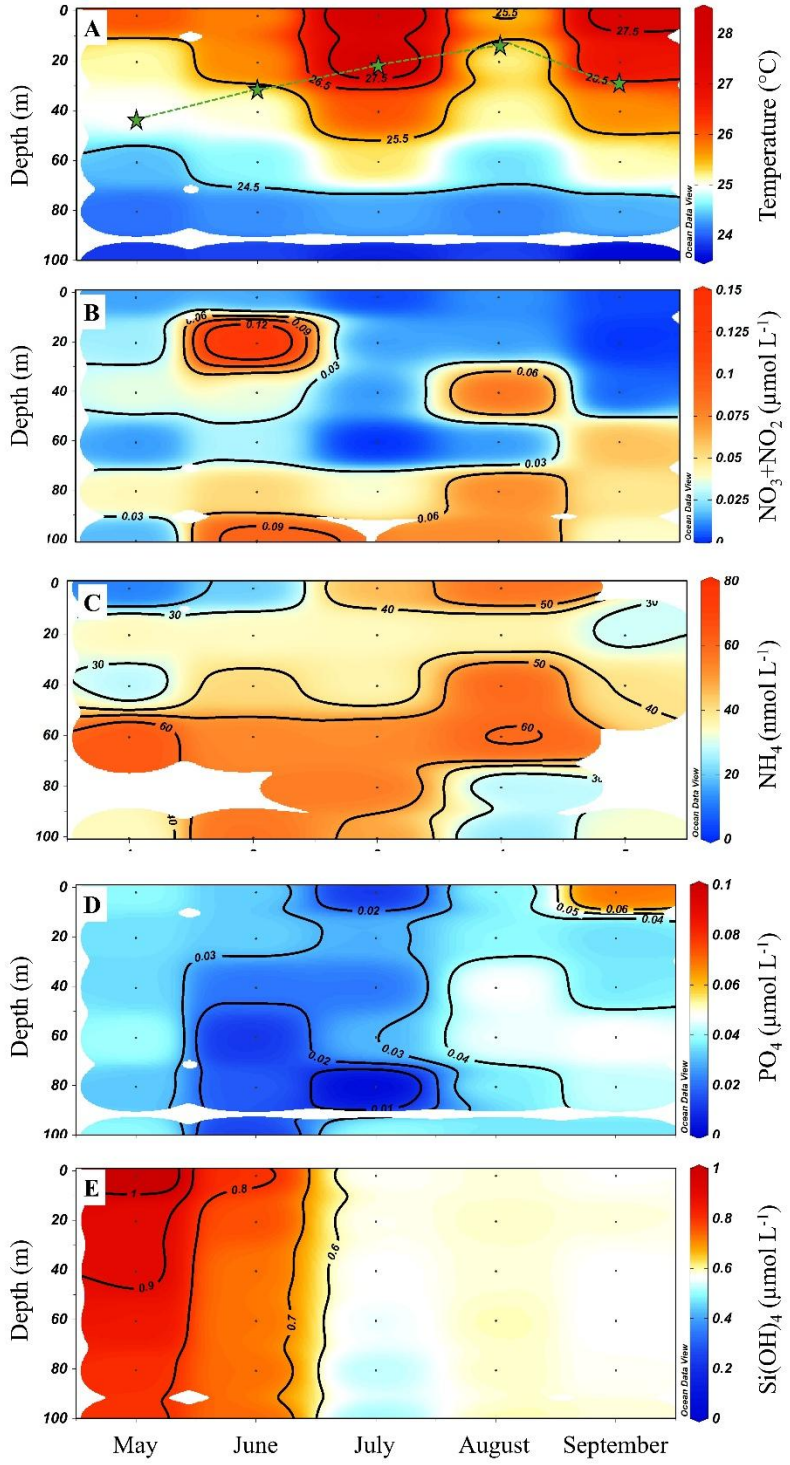

325

326 **Figure 1**: Depth distribution of temperature (A), NO_2+NO_3 (B), NH_4 (C), PO_4 (D) and $Si(OH)_4$
327 (E) in the upper water column (0-100 m) of the Gulf of Aqaba during summertime (May to
328 September). The green star in panel A signifies the MLD (more information in Table 1).

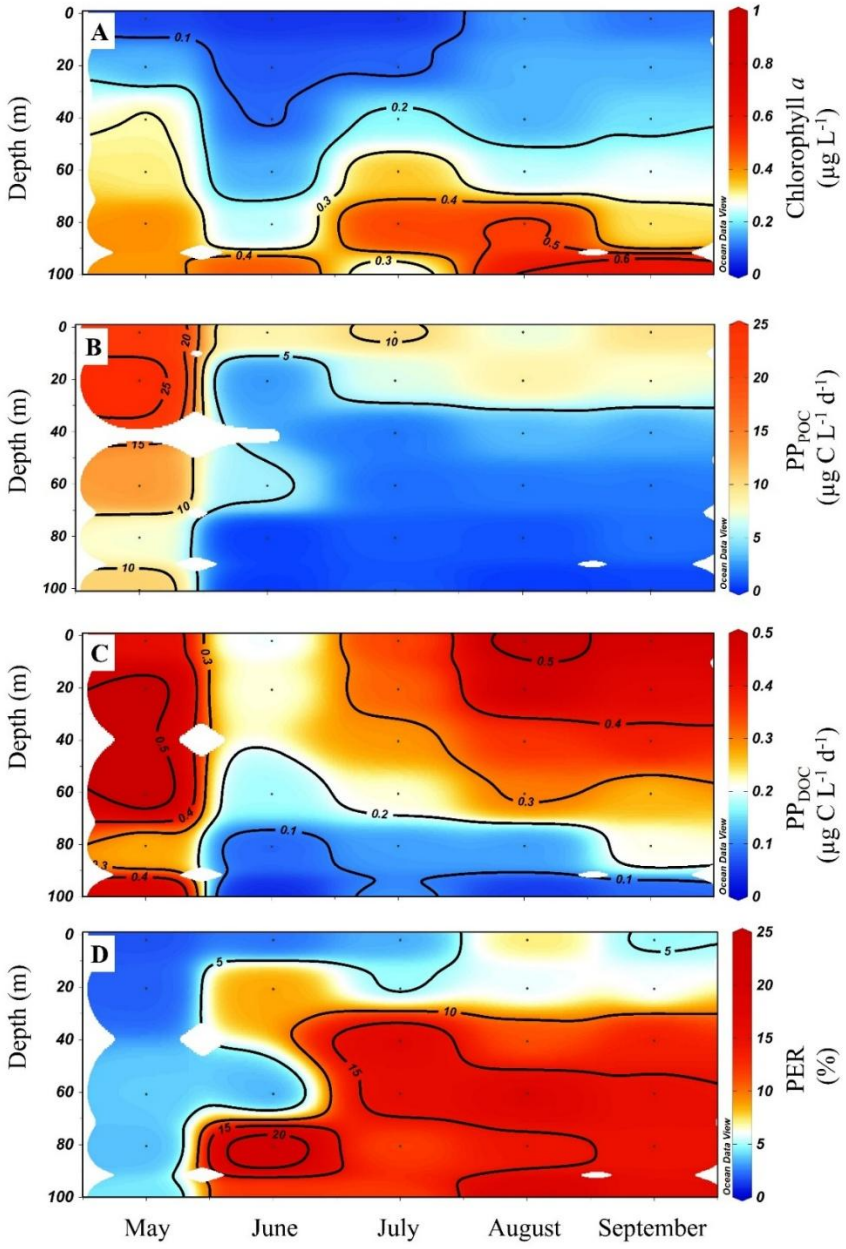

329

330 **Figure 2**: Depth distribution of chlorophyll *a* (A), PP_{POC} (B) PP_{DOC} (C) and the percentage of
331 extracellular release, PER (D) in the upper water column (0-100 m) of the Gulf of Aqaba during
332 summertime (May to September).

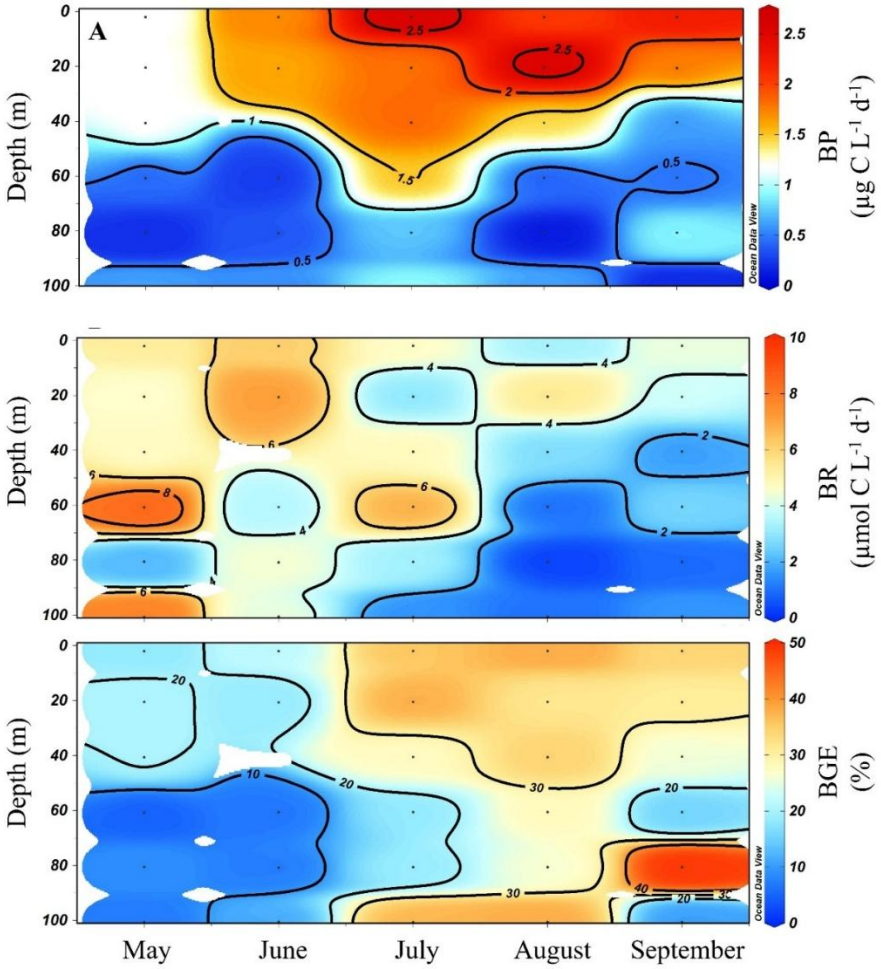

333

334 **Figure 3**: Depth distribution of bacterial productivity, BP (A), bacterial respiration, BR (B),
335 and bacterial gross efficiency, BGE (C) in the upper water column (0-100 m) of the Gulf of
336 Aqaba during summertime (May to September).

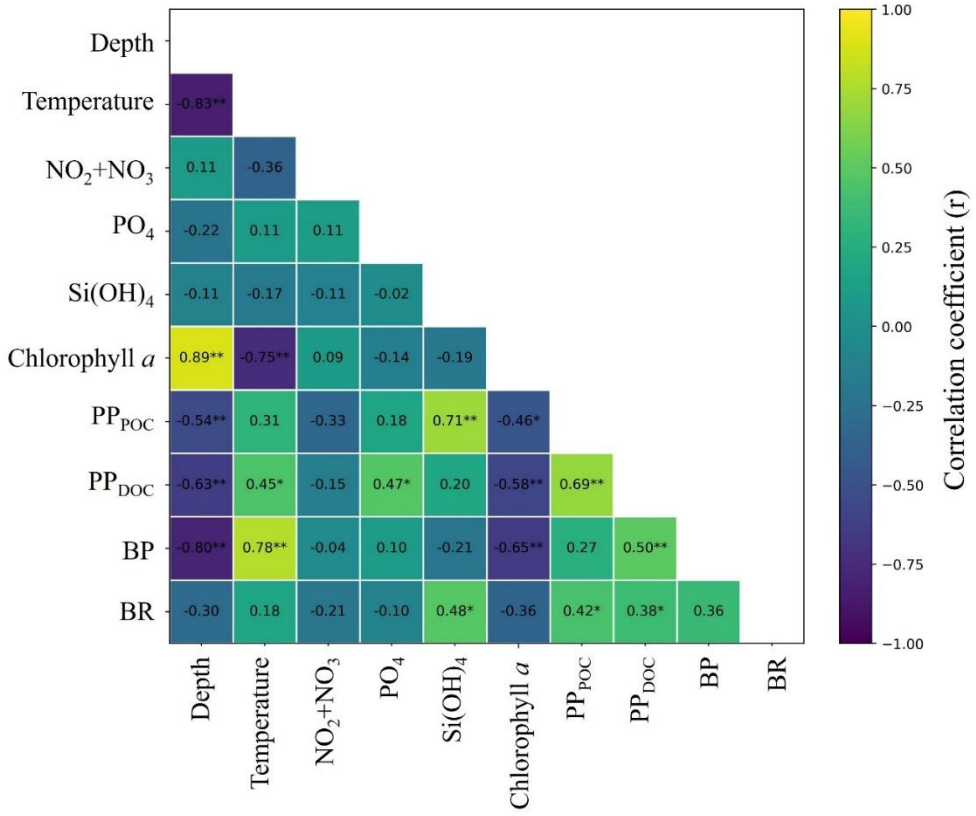

337

338 **Figure 4**: Pearson correlation matrix of physical, chemical, and biological variables measured
339 in the upper 0–100 m of the water column. Colores indicate the strength and direction of the
340 correlation (Pearson's r), and values within each cell represent correlation coefficients.
341 Statistical significance is indicated as *p<0.05 and **p<0.01. The analysis is based on all
342 depth-resolved measurements across the five cruises (May to September).

343 **Table 1**: Summary of integrated values (0-100 m) measured in the Gulf of Aqaba during the
344 summer.

	May	June	July	August	September
Mixed layer depth (m)	45	31	21	15	28
% of surface irradiance at 100 m	1.3	0.8	0.6	1.8	1.5
NO_3+NO_2 (μmol m^{-2})	4.5	11.2	7.5	7.8	6.0
NH_4 (μmol m^{-2})	1.7	4.5	4.6	3.4	3.0
PO_4 (μmol m^{-2})	3.5	2.1	2.1	4.1	4.3
DIN/PO_4 (ratio)*	1.8	7.5	5.8	2.7	2.1
$Si(OH)_4$ (μmol m^{-2})	89	75	55	59	57
PP_{POC} (g C m^{-2} d^{-1})	1.26	0.28	0.34	0.37	0.39
PP_{DOC} (g C m^{-2} d^{-1})	0.03	0.02	0.02	0.03	0.03
PER (%)	2.5	5.7	5.6	6.4	7.4
BP (g C m^{-2} d^{-1})	0.08	0.08	0.16	0.12	0.10
CR (g C m^{-2} d^{-1})	1.03	1.01	0.86	0.50	0.53
BR (g C m^{-2} d^{-1})	0.52	0.51	0.42	0.23	0.24
BGE (%)	13.5	13.1	27.7	34.1	29.8
PP_{TOT}/CR (ratio)**	1.26	0.30	0.42	0.78	0.78

345 * DIN = NH_4+NO_3+NO_2
346 ** PP_{TOT} = PP_{POC}+PP_{DOC}

4. Discussion

4.1. Summer stratification shifts carbon cycling toward dissolved pathways

The Gulf of Aqaba exhibits strong seasonal hydrographic variability with deep winter mixing followed by stable stratification afterward (Biton and Gildor, 2011), leading to nutrient-depleted surface water throughout the summer months (Laiolo et al., 2014; Efrat Meeder et al., 2012). The shift from deeply mixed winter conditions to a strongly stratified summer water column substantially reshapes autotrophic production, heterotrophic activity, and the efficiency with which carbon is exported from the surface (Karl et al., 2021). Understanding how microbial communities adjust their carbon-use strategies under nutrient-poor conditions is therefore important for predicting the fate of newly fixed carbon in stratified and oligotrophic oceans.

The progressive shoaling of the mixed layer from early to late summer (Table 1), together with persistently low nutrient concentrations and reduced nutrient inventories (Figure 1B-E), indicates increasing isolation of the euphotic zone from the nutricline, typically located at depths >150 m in this region (Landou et al., 2023; Meeder et al., 2012; Rahav et al., 2015). As stratification intensified, depth-integrated primary production declined from early to mid-summer, while chlorophyll biomass became increasingly concentrated within a pronounced DCM (Figure 2A). This decoupling between biomass and productivity is consistent with a community persisting under chronic low light and low nutrient availability (Marañón et al., 2010), representing a deep photo-acclimation maximum (DAM) rather than a deep biomass maximum (DBM) as found in some other oligotrophic settings (Hodges and Rudnick, 2004; Mignot et al., 2014). Additionally, the sharp decline in heterotrophic BP with depth (Figure 3A) likely reduces microbial loss rates, thereby allowing photo-acclimated phytoplankton at the DCM (mainly *Prochlorococcus*, Lindell and Post, 1995; Reich et al., 2024) to persist despite low carbon fixation rates. In other words, the high chlorophyll does not imply high biomass but rather high chlorophyll content per cell. At the same time, the vertical distributions of PP_{DOC} and PER indicate a shift in carbon allocation within the water column (Figure 2). PP_{DOC} remains concentrated in the upper water column and is relatively stable over the season, while PER increases both with depth and over time, reaching its highest values during periods of strongest stratification (Figure 2). This pattern implies that an increasing fraction of newly fixed carbon was released as DOC in the upper 100 m, especially as summer progressed and as imbalances between carbon fixation and nutrient assimilation limited biomass synthesis and 'favored' the exudation of photosynthates (Mueller et al., 2016; Ofaim et al., 2021). Under such conditions, excess carbon leaks or excreted as low-molecular-weight compounds, thus

elevating PER and enhancing the supply of labile dissolved organic substrates to heterotrophic prokaryotes (Engel et al., 2017, 2014, 2004). Consequently, a larger share of PP_{TOT} was routed into the microbial loop rather than retained in particulate autotrophic biomass (i.e., PP_{POC}), enhancing carbon recycling and reducing the efficiency of export to depth (Table 1; Carlson et al., 2010).

The increasing release of newly fixed carbon as dissolved organic matter thus provides a key link between autotrophic production and sustained heterotrophic activity within the euphotic zone, even as primary production declines over the summer (Table 1, Figure 2). In oligotrophic systems such as the Gulf of Aqaba, heterotrophic microbial communities are often tightly coupled to DOC supply derived from contemporaneous primary production as well as semi-labile DOC that accumulates over seasonal timescales (Hansell et al., 2009; Santinelli, 2015). The persistence of BP in our study suggests that microbial metabolism is supported by a combination of freshly released DOC, recycled organic matter, and/or external nutrient inputs such as those added from aerosol deposition (Paytan et al., 2009; Rahav et al., 2018). Similar accumulated DOC and associated impacts on the microbial community have been observed in other stratified regions (Hansell et al., 2009; Hansell and Carlson, 2002). In contrast, a recent study in the Eastern Tropical North Atlantic reported that BP and BR closely follow PP_{TOT}, with PP_{DOC} supply often exceeded bacterial carbon demand (Devresse et al., 2022). There, heterotrophic activity was largely controlled by and coupled to contemporaneous production, resulting in a production-driven carbon cycle. In the Gulf of Aqaba, however, the weaker coupling between PP_{TOT} and heterotrophic activity points to a recycling-dominated regime in which microbial communities increasingly depend on internally regenerated carbon and are not directly linked to contemporaneous production. Under sustained stratification, reduced nutrient supply constrains autotrophic growth while promoting DOC release and accumulation, thereby maintaining BR even as primary production declines (Hansell et al., 2009; Hansell, 2013). Interestingly, while absolute rates of PP_{DOC} significantly correlate with bacterial production ($r=0.50$, $p<0.01$; Figure 4), the PER does not exhibit a statistically significant correlation with BGE across the water column ($r=0.106$, $p=0.59$). This decoupling is primarily driven by opposing vertical gradients, as PER increases toward the base of the euphotic zone while BGE peaks in warmer surface layers, as well as potential bacterial overflow metabolism where carbon-rich exudates are preferentially respired rather than assimilated into biomass. Nevertheless, the low BGE observed (Table 1, Figure 3C) further support the view that most of the consumed carbon is respired rather than converted into biomass, a characteristic of strongly recycling systems in oligotrophic ocean settings (del Giorgio and Cole, 1998). Indeed,

the vertical structure of BGE closely mirrors that of BR, indicating that most of the organic carbon processed by heterotrophic prokaryotes was respired rather than incorporated into new biomass. These low growth efficiencies are consistent with the energetic constraints typical of oligotrophic waters, indicating that bacterial carbon use was directed mainly toward respiration rather than growth, with much of the organic carbon rapidly returned to dissolved inorganic form (del Giorgio and Cole, 1998). These low growth efficiencies are consistent with the energetic constraints typical of highly stratified oligotrophic waters, indicating that bacterial carbon use was directed mainly toward respiration rather than growth, with much of the organic carbon rapidly returned to dissolved inorganic form (del Giorgio and Cole, 1998). While low BGE is widely observed in unproductive open-ocean settings, a recent study from the oligotrophic Taiwan Strait reported elevated BGE values (Liu et al., 2026). Such contrasts suggest that oligotrophy alone does not dictate bacterial metabolic efficiency. Instead, BGE may be regulated by the substrate stoichiometry and lability, thermal regimes, and different physical oceanographic settings. In systems exhibiting higher BGE such as the Taiwan Strait, heterotrophic bacteria may access labile dissolved organic matter or nutrient-rich substrates through micro-scale spatial patchiness (e.g., phycosphere exudates, viral lysis), rapid biological turnover, or episodic physical events like upwelling, terrestrial runoff, and Kuroshio intrusions (Liu et al., 2026). In contrast, in the hyper-oligotrophic, warm, and highly isolated summer water column of the Gulf of Aqaba, severe nutrient limitation likely promotes the exudation of carbon-rich, nutrient-poor dissolved organic matter. This forces heterotrophic bacteria to respire excess carbon via overflow metabolism to meet their nutritional demands while sustaining high basal metabolic costs, thereby maintaining low to moderate BGE.

We acknowledge that the nominal ~0.7 μm pore size of GF/F filters may raise concerns regarding the potential passage of small picoplankton, particularly *Prochlorococcus*. However, previous studies indicate that cell breakthrough is minimal under low-vacuum filtration conditions. For example, Bertilsson et al., (2003) showed that ~95% of cells in an axenic culture of *Prochlorococcus marinus* MED4 were retained on Whatman GF/F filters under low vacuum, comparable to the conditions and filters used in our study. In addition, although not specifically addressing *Prochlorococcus*, Chavez et al., (1995) reported equivalent recovery of total chlorophyll a using GF/F and 0.2 μm membrane filters in oligotrophic open-ocean samples, suggesting that GF/F filtration is unlikely to result in substantial loss of phytoplankton biomass (and thus production) under similar conditions. Moreover, the observed seasonal increase in PER (Figure 2D) was associated with changes in nutrient availability and microbial metabolism rather than simply tracking chlorophyll biomass. These observations therefore

support the interpretation that the increase in extracellular release reflects a physiological response rather than an artifact of size-selective filtration. Additionally, abiotic retention or adsorption of ^{14}C-labeled dissolved organic matter onto the glass-fiber matrix may lead to biased PP_{POC} and, consequently, of PER (López-Sandoval et al., 2018; Maske and Garcia-Mendoza, 1994). Nevertheless, the shift toward elevated PP_{DOC} and PER as summer stratification progress, despite this potential matrix adsorption, suggest that enhanced extracellular release is a genuine physiological feature of nutrient-stressed autotrophs in the study area rather than a filtration artifact.

4.2. Potential drivers of microbial carbon processing in the Gulf of Aqaba during summertime

The observed vertical patterns in microbial carbon cycling are primarily structured by gradients in light availability/nutrient supply and stratification intensity, which all co-vary with depth (Figure 4). Chlorophyll *a* peaks at the DCM, reflecting photo-acclimated cells at depth (DAM), while rates of PP_{TOT}, PP_{DOC}, and BP are highest in the upper, well-lit layers. Within this framework, a strong coupling between PP_{POC} and PP_{DOC} would suggest that dissolved carbon release scales directly with photosynthetic activity, consistent with extracellular release as an inherent component of primary production under oligotrophic conditions. However, the negative relationship between both PP_{POC} and PP_{DOC} with chlorophyll *a* (Figure 4) indicates that carbon fixation and release are not directly linked to standing stock of biomass, but rather to physiological activity in the upper water column (Figure 2). Importantly, PP_{DOC} showed a stronger association with BP than PP_{POC} does, emphasizing the central role of dissolved organic carbon in sustaining heterotrophic metabolism. This supports the idea that the microbial loop in the Gulf of Aqaba is primarily fueled by recently produced dissolved substrates rather than by particulate pathways (abovementioned references). The absence of strong linear correlations between ambient nutrient concentrations and biological rates reflects the rapid uptake capacity of nutrient-starved microbial communities. This rapid biological drawdown maintains nutrient pools near detection limits, effectively masking statistical correlations. Together, these patterns indicate that carbon cycling in the Gulf of Aqaba is structured by two complementary processes: (i) vertical decoupling between biomass accumulation and carbon cycling activity driven by stratification, and (ii) tight coupling between dissolved carbon production and heterotrophic utilization (Figure 4).

5. Conclusions

Our observations provide a quantitative and process-based framework for understanding how stratification restructures carbon flow, showing that the Gulf of Aqaba system shifts from particulate production toward sustained dissolved carbon release that maintains heterotrophic metabolism despite declining primary production. As climate-driven warming intensifies the density barriers of low- and mid-latitude pelagic systems (Duarte et al., 2013), nutrient recycling rates are expected to become more prevalent, potentially enhancing DOC turnover, thus lowering carbon export efficiency, and strengthening the role of the microbial loop in regulating air-sea CO_2 exchange. Thus, increased stratification may lead to longer residence times of organic carbon in the surface ocean (through multiple regeneration and utilization cycles), tighter microbial coupling to DOC, and an expansion of BR relative to BP, with implications for nutrient regeneration, and ecosystem structure, including shifts toward smaller phytoplankton and more efficient recyclers.

Future work should explicitly link physical forcing, nutrient inputs, and microbial carbon partitioning across seasonal to interannual scales in the Gulf of Aqaba and other oligotrophic basins. Long-term observations and targeted experiments that manipulate stratification, nutrient supply, and temperature will be essential to predict how microbial communities adjust DOC release, BGE, and BR under progressing oligotrophication. Integrating field measurements with trait-based and ecosystem models could help quantify how shifts in microbial carbon dynamics under enhanced stratification alter the efficiency of the biological carbon pump and feedback to climate, including potential interactions with aerosol inputs and emerging stressors such as acidification and deoxygenation.

Data Availability Statement

All the data is presented in the graphs/table/text and will be made available in excel format upon request.

Credit Authorship Contribution Statement

Conceptualized; ER. Data curation, formal analysis, and visualization; ER, and AP. The paper was prepared and revised by ER and AP.

Acknowledgments

The authors thank the personnel from the Israeli National Monitoring project of Eilat and the Inter University Institute for Marine Sciences in Eilat (IUI) and to two anonymous reviewers that helped clarifying and reshaping the manuscript.

Funding

This paper was partly supported by a grant from the Middle East Regional Cooperation (MERC) (M39-011) to ER and AP and by the Israel Science Foundation (grant no. 821/22) to ER.

References

Alkalay, R., Zlatkin, O., Katz, T., Herut, B., Halicz, L., Berman-Frank, I., Weinstein, Y., 2020. Carbon export and drivers in the southeastern Levantine Basin. Deep. Res. Part II Top. Stud. Oceanogr. 171, 104713. https://doi.org/10.1016/j.dsr2.2019.104713

Alothman, A., Duarte, C.M., Qurban, M.A., Agustí, S., 2025. Flow of heterotrophic production in oligotrophic ocean waters. Front. Microbiol. 16, 1530627. https://doi.org/10.3389/fmicb.2025.1530627

Anderson, T.R., Turley, C.M., 2003. Low bacterial growth efficiency in the oligotrophic eastern Mediterranean Sea: a modelling analysis. J. Plankton Res. 25, 1011–1019. https://doi.org/10.1093/plankt/25.9.1011

Aranguren-Gassis, M., Teira, E., Serret, P., Martínez-García, S., Fernández, E., 2012. Potential overestimation of bacterial respiration rates in oligotrophic plankton communities. Mar. Ecol. Prog. Ser. 453, 1–10.

Armengol, L., Calbet, A., Franchy, G., Rodríguez-Santos, A., Hernández-León, S., 2019. Planktonic food web structure and trophic transfer efficiency along a productivity gradient in the tropical and subtropical Atlantic Ocean. Sci. Rep. 9, 2044. https://doi.org/10.1038/s41598-019-38507-9

Avrahami, Y., Koplovitz, G., Frada, M.J., 2025. Diatom community succession and bloom variability as a function of winter-mixing depth in the subtropical Gulf of Aqaba, Red Sea. Mar. Ecol. Prog. Ser. 760, 39–54.

Azam, F., Malfatti, F., 2007. Microbial structuring of marine ecosystems. Nat. Rev. Microbiol. 5, 782–91. https://doi.org/10.1038/nrmicro1747

Baetge, N., Behrenfeld, M.J., Fox, J., Halsey, K.H., Mojica, K.D.A., Novoa, A., Stephens, B.M., Carlson, C.A., 2021. The seasonal flux and fate of dissolved organic carbon through bacterioplankton in the Western North Atlantic. Front. Microbiol. 12, 669883. https://doi.org/10.3389/fmicb.2021.669883

Bertilsson, S., Berglund, O., Karl, D.M., Chisholm, S.W., 2003. Elemental composition of marine Prochlorococcus and Synechococcus: Implications for the ecological

550 stoichiometry of the sea. Limnol. Oceanogr. 48, 1721–1731.
551 https://doi.org/10.4319/lo.2003.48.5.1721
552 Biton, E., Gildor, H., 2011. The general circulation of the Gulf of Aqaba (Gulf of Eilat)
553 revisited: The interplay between the exchange flow through the Straits of Tiran and
554 surface fluxes. J. Geophys. Res. 116, 1–15. https://doi.org/10.1029/2010JC006860
555 Carlson, C.A., Hansell, D.A., Nelson, N.B., Siegel, D.A., Smethie, W.M., Khatiwala, S.,
556 Meyers, M.M., Halewood, E., 2010. Dissolved organic carbon export and subsequent
557 remineralization in the mesopelagic and bathypelagic realms of the North Atlantic basin.
558 Deep Sea Res. Part II Top. Stud. Oceanogr. 57, 1433–1445.
559 https://doi.org/https://doi.org/10.1016/j.dsr2.2010.02.013
560 Chavez, F.P., Buck, K.R., Bidigare, R.R., Karl, D.M., Hebel, D., Latasa, M., Campbell, L.,
561 Newton, J., 1995. On the chlorophyll a retention properties of glass-fiber GF/F filters.
562 Limnol. Oceanogr. 40, 428–433.
563 https://doi.org/https://doi.org/10.4319/lo.1995.40.2.0428
564 Chen, Z., Sun, J., Gu, T., Zhang, G., Wei, Y., 2021. Nutrient ratios driven by vertical
565 stratification regulate phytoplankton community structure in the oligotrophic western
566 Pacific Ocean. Ocean Sci. 17, 1775–1789. https://doi.org/10.5194/os-17-1775-2021
567 Cheung, H.L.S., Simister, R.L., Not, C., Crowe, S.A., 2024. Microbial community respiration
568 kinetics and their dynamics in coastal seawater. Sci. Total Environ. 954, 176119.
569 https://doi.org/https://doi.org/10.1016/j.scitotenv.2024.176119
570 Dave, A.C., Lozier, M.S., 2010. Local stratification control of marine productivity in the
571 subtropical North Pacific. J. Geophys. Res. Ocean. 115.
572 https://doi.org/https://doi.org/10.1029/2010JC006507
573 de Boyer Montégut, C., Madec, G., Fischer, A.S., Lazar, A., Iudicone, D., 2004. Mixed layer
574 depth over the global ocean: An examination of profile data and a profile-based
575 climatology. J. Geophys. Res. Ocean. 109, C12003.
576 https://doi.org/https://doi.org/10.1029/2004JC002378
577 del Giorgio, P. a., Cole, J.J., 1998. Bacterial growth efficiency in natural aquatic systems.
578 Annu. Rev. Ecol. Syst. 29, 503–541. https://doi.org/10.1146/annurev.ecolsys.29.1.503
579 del Giorgio, P., Cole, J.J., Cimbleris, A., 1997. Respiration rates in bacteria exceed
580 phytoplankton production in unproductive aquatic systems. Nature 385, 148–151.
581 Devresse, Q., Becker, K.W., Bendinger, A., Hahn, J., Engel, A., 2022. Eddy-enhanced
582 primary production sustains heterotrophic microbial activities in the Eastern Tropical
583 North Atlantic. Biogeosciences 19, 5199–5219. https://doi.org/10.5194/bg-19-5199-

584 2022
585 Dore, J.E., Letelier, R.M., Church, M.J., Lukas, R., Karl, D.M., 2008. Summer phytoplankton
586 blooms in the oligotrophic North Pacific Subtropical Gyre: Historical perspective and
587 recent observations. Prog. Oceanogr. 76, 2–38.
588 https://doi.org/https://doi.org/10.1016/j.pocean.2007.10.002
589 Duarte, C.M., Duarte, C.M., Regaudie-de-gioux, A., Agust, S., 2013. The oligotrophic ocean
590 is heterotrophic. Ann. Rev. Mar. Sci. 5, 551–569. https://doi.org/10.1146/annurev-
591 marine-121211-172337
592 Engel, A., Bange, H.W., Cunliffe, M., Burrows, S.M., Friedrichs, G., Galgani, L., Herrmann,
593 H., Hertkorn, N., Johnson, M., Liss, P.S., Quinn, P.K., Schartau, M., Soloviev, A.,
594 Stolle, C., Upstill-Goddard, R.C., van Pinxteren, M., Zäncker, B., 2017. The Ocean's
595 Vital Skin: Toward an Integrated Understanding of the Sea Surface Microlayer. Front.
596 Mar. Sci. 4. https://doi.org/10.3389/fmars.2017.00165
597 Engel, A., Piontek, J., Grossart, H.P., Riebesell, U., Schulz, K.G., Sperling, M., 2014. Impact
598 of CO2 enrichment on organic matter dynamics during nutrient induced coastal
599 phytoplankton blooms. J. Plankton Res. 36, 641–657.
600 https://doi.org/10.1093/plankt/fbt125
601 Engel, A., Thoms, S., Riebesell, U., Rochelle-Newall, E., Zondervan, I., 2004.
602 Polysaccharide aggregation as a potential sink of marine dissolved organic carbon.
603 Nature 428, 929–932. https://doi.org/10.1038/nature02453
604 Hansell, D., Carlson, C.A., Repeta, D.J., Schlitzer, R., 2009. Dissolved Organic Matter in the
605 Ocean. Oceanography 22, 202–11. https://doi.org/10.5670/oceanog.2009.109
606 Hansell, D.A., 2013. Recalcitrant Dissolved Organic Carbon Fractions. Ann. Rev. Mar. Sci.
607 5, 421–445. https://doi.org/10.1146/annurev-marine-120710-100757
608 Hansell, D.A., Carlson, C.A., 2002. Biogeochemistry of marine dissolved organic matter.
609 Academic Press, New York. https://doi.org/10.1016/B978-0-12-323841-2.X5000-3
610 Hazan, O., Silverman, J., Sisma-Ventura, G., Ozer, T., Gertman, I., Shoham-Frider, E., Kress,
611 N., Rahav, E., 2018. Mesopelagic prokaryotes alter surface phytoplankton production
612 during simulated deep mixing experiments in Eastern Mediterranean Sea waters. Front.
613 Mar. Sci. 5, 1. https://doi.org/10.3389/fmars.2018.00001
614 Hodges, B.A., Rudnick, D.L., 2004. Simple models of steady deep maxima in chlorophyll
615 and biomass. Deep Sea Res. Part I Oceanogr. Res. Pap. 51, 999–1015.
616 https://doi.org/https://doi.org/10.1016/j.dsr.2004.02.009
617 Holms, R.., Aminot, A., Kérouel, R., Hooker, B.., Peterson, B.., 1999. A simple and precise

618 method for measuring ammonium in marine and freshwater ecosystems. Can. Data Rep.
619 Fish. Aquat. Sci. 56, 1801–1808. https://doi.org/10.1139/cjfas-56-10-1801
620 Iluz, D., Dishon, G., Capuzzo, E., Meeder, E., Astoreca, R., Montecino, V., Znachor, P.,
621 Ediger, D., Marra, J., 2009. Short-term variability in primary productivity during a
622 wind-driven diatom bloom in the Gulf of Eilat (Aqaba). Aquat. Microb. Ecol. 56, 205–
623 215. https://doi.org/10.3354/ame01321
624 Izett, R.W., Fennel, K., Stoer, A.C., Nicholson, D.P., 2024. Reviews and syntheses:
625 expanding the global coverage of gross primary production and net community
626 production measurements using Biogeochemical-Argo floats. Biogeosciences 21, 13–47.
627 https://doi.org/10.5194/bg-21-13-2024
628 Kang, J., Luo, Z., Mohamed, H.F., Lin, Y., Huang, S., Wang, Y., Lan, W., 2022.
629 Environmental Regulation of Photosynthetically Produced Dissolved Organic Carbon by
630 Phytoplankton Along a Subtropical Estuarine Bay. Front. Mar. Sci. 9, 13401.
631 https://doi.org/10.3389/fmars.2022.813401
632 Karl, D.M., Letelier, R.M., Bidigare, R.R., Björkman, K.M., Church, M.J., Dore, J.E., White,
633 A.E., 2021. Seasonal-to-decadal scale variability in primary production and particulate
634 matter export at Station ALOHA. Prog. Oceanogr. 195, 102563.
635 https://doi.org/https://doi.org/10.1016/j.pocean.2021.102563
636 Kress, N., Herut, B., 2001. Spatial and seasonal evolution of dissolved oxygen and nutrients
637 in the Southern Levantine Basin (Eastern Mediterranean Sea): chemical
638 characterization of the water masses and inferences on the N : P ratios. Deep. Res. I 48,
639 2347–2372.
640 Krom, M.D., Woodward, E.M.S., Herut, B., Kress, N., Carbo, P., Mantoura, R.F.C., Spyres,
641 G., Thingsted, T.F., Wassmann, P., Wexels-Riser, C., Kitidis, V., Law, C., Zodiatis, G.,
642 2005. Nutrient cycling in the south east Levantine basin of the eastern Mediterranean:
643 Results from a phosphorus starved system. Deep. Res. Part II Top. Stud. Oceanogr. 52,
644 2879–2896. https://doi.org/10.1016/j.dsr2.2005.08.009
645 LaBrie, R., Péquin, B., Fortin St-Gelais, N., Yashayaev, I., Cherrier, J., Gélinas, Y.,
646 Guillemette, F., Podgorski, D.C., Spencer, R.G.M., Tremblay, L., Maranger, R., 2022.
647 Deep ocean microbial communities produce more stable dissolved organic matter
648 through the succession of rare prokaryotes. Sci. Adv. 8, eabn0035.
649 https://doi.org/10.1126/sciadv.abn0035
650 Laiolo, L., Barausse, A., Dubinsky, Z., Palmeri, L., Goffredo, S., Kamenir, Y., Al-Najjar, T.,
651 Iluz, D., 2014. Phytoplankton dynamics in the Gulf of Aqaba (Eilat, Red Sea): A

652 simulation study of mariculture effects. Mar. Pollut. Bull. 86, 481–493.
653 https://doi.org/https://doi.org/10.1016/j.marpolbul.2014.06.026
654 Landou, E., Lazar, B., LaRoche, J., Fennel, K., Berman-Frank, I., 2023. Contribution of
655 photic and aphotic N2 fixation to production in an oligotrophic sea. Limnol. Oceanogr.
656 68, 692–708. https://doi.org/10.1002/lno.12303
657 Lindell, D., Post, A.F., 1995. Ultraphytoplankton succession is triggered by deep winter
658 mixing in the Gulf of Aqaba (Eilat), Red Sea. Limnol. Oceanogr. 40, 1130–1141.
659 https://doi.org/10.4319/lo.1995.40.6.1130
660 Liu, Y., Kang, J., Huang, Y., Xue, C., Huang, B., 2026. Linking phytoplankton-derived
661 dissolved and particulate carbon production to bacterial metabolism across physical
662 dynamics in a subtropical marginal sea. J. Geophys. Res. Ocean. 131, e2026JC024071.
663 https://doi.org/https://doi.org/10.1029/2026JC024071
664 López-Sandoval, D.C., Delgado-Huertas, A., Agustí, S., 2018. The 13C method as a robust
665 alternative to 14C-based measurements of primary productivity in the Mediterranean
666 Sea. J. Plankton Res. 40, 544–554. https://doi.org/10.1093/plankt/fby031
667 Lozier, M.S., Dave, A.C., Palter, J.B., Gerber, L.M., Barber, R.T., 2011. On the relationship
668 between stratification and primary productivity in the North Atlantic. Geophys. Res.
669 Lett. 38. https://doi.org/https://doi.org/10.1029/2011GL049414
670 Marañón, E., Behrenfeld, M.J., González, N., Mouriño, B., Zubkov, M. V., 2003. High
671 variability of primary production in oligotrophic waters of the Atlantic Ocean:
672 Uncoupling from phytoplankton biomass and size structure. Mar. Ecol. Prog. Ser. 257,
673 1–11. https://doi.org/10.3354/meps257001
674 Marañón, E., Fernández, A., Mouriño-Carballido, B., Martínez-García, S., Teira, E.,
675 Cermeño, P., Chouciño, P., Huete-Ortega, M., Fernández, E., Calvo-Díaz, A., Anxelu G.
676 Morán, X., Bode, A., Moreno-Ostos, E., Varela, M.M., Patey, M.D., Achterberg, E.P.,
677 2010. Degree of oligotrophy controls the response of microbial plankton to Saharan
678 dust. Limnol. Oceanogr. 55, 2339–2352. https://doi.org/10.4319/lo.2010.55.6.2339
679 Maske, H., Garcia-Mendoza, E., 1994. Adsorption of dissolved organic matter to the
680 inorganic filter substrate and its implications for C uptake measurements. Appl. Environ.
681 Microbiol. 60, 3887–3889. https://doi.org/10.1128/aem.60.10.3887-3889.1994
682 Meeder, Efrat, MacKey, K.R.M., Paytan, A., Shaked, Y., Iluz, D., Stambler, N., Rivlin, T.,
683 Post, A.F., Lazar, B., 2012. Nitrite dynamics in the open ocean-clues from seasonal and
684 diurnal variations. Mar. Ecol. Prog. Ser. 453, 11–26. https://doi.org/10.3354/meps09525
685 Mentges, A., Feenders, C., Deutsch, C., Blasius, B., Dittmar, T., 2019. Long-term stability of

686 marine dissolved organic carbon emerges from a neutral network of compounds and
687 microbes. Sci. Rep. 9, 17780. https://doi.org/10.1038/s41598-019-54290-z
688 Mignot, A., Claustre, H., Uitz, J., Poteau, A., D'Ortenzio, F., Xing, X., 2014. Understanding
689 the seasonal dynamics of phytoplankton biomass and the deep chlorophyll maximum in
690 oligotrophic environments: A Bio-Argo float investigation. Global Biogeochem. Cycles
691 28, 856–876. https://doi.org/https://doi.org/10.1002/2013GB004781
692 Morana, C., Sarmento, H., Descy, J.-P., Gasol, J.M., Borges, A. V, Bouillon, S.,
693 Darchambeau, F., 2014. Production of dissolved organic matter by phytoplankton and its
694 uptake by heterotrophic prokaryotes in large tropical lakes. Limnol. Oceanogr. 59,
695 1364–1375. https://doi.org/https://doi.org/10.4319/lo.2014.59.4.1364
696 Mueller, B., den Haan, J., Visser, P.M., Vermeij, M.J.A., van Duyl, F.C., 2016. Effect of light
697 and nutrient availability on the release of dissolved organic carbon (DOC) by Caribbean
698 turf algae. Sci. Rep. 6, 23248. https://doi.org/10.1038/srep23248
699 Ofaim, S., Sulheim, S., Almaas, E., Sher, D., Segrè, D., 2021. Dynamic allocation of carbon
700 storage and nutrient-dependent exudation in a revised genome-gcale model of
701 Prochlorococcus. Front. Genet. 12, 586293. https://doi.org/10.3389/fgene.2021.586293
702 Paytan, A., Mackey, K.R.M., Chen, Y., Lima, I.D., Doney, S.C., Mahowald, N., Labiosa, R.,
703 Post, A.F.A.F., 2009. Toxicity of atmospheric aerosols on marine phytoplankton. Proc.
704 Natl. Acad. Sci. U. S. A. 106, 4601–5. https://doi.org/10.1073/pnas.0811486106
705 Pennington, J.T., Mahoney, K.L., Kuwahara, V.S., Kolber, D.D., Calienes, R., Chavez, F.P.,
706 2006. Primary production in the eastern tropical Pacific: A review. Prog. Oceanogr. 69,
707 285–317. https://doi.org/https://doi.org/10.1016/j.pocean.2006.03.012
708 Polovina, J.J., Howell, E. a., Abecassis, M., 2008. Ocean's least productive waters are
709 expanding. Geophys. Res. Lett. 35, 2–6. https://doi.org/10.1029/2007GL031745
710 Rahav, E., Giannetto, M., Bar-Zeev, E., 2016. Contribution of mono and polysaccharides to
711 heterotrophic N2 fixation at the eastern Mediterranean coastline. Sceintific Reports 6,
712 27858. https://doi.org/10.1038/srep27858
713 Rahav, E, Herut, B., Mulholland, M., Belkin, N., Elifantz, H., Berman-Frank, I., 2015.
714 Heterotrophic and autotrophic contribution to dinitrogen fixation in the Gulf of Aqaba.
715 Mar. Ecol. Prog. Ser. 522, 67–77. https://doi.org/10.3354/meps11143
716 Rahav, E., Paytan, A., Mescioglu, E., Galletti, Y., Rosenfeld, S., Raveh, O., Santinelli, C.,
717 Ho, T.Y., Herut, B., 2018. Airborne Microbes Contribute to N2 Fixation in Surface
718 Water of the Northern Red Sea. Geophys. Res. Lett. 45, 6186–6194.
719 https://doi.org/10.1029/2018GL077132

Rahav, E., Wankel, S.D., Paytan, A., 2026. Ammonia and nitrite oxidation in the upper euphotic zone of the oligotrophic Red Sea. Biogeosciences 23, 4171–4185. https://doi.org/10.5194/bg-23-4171-2026

Redfield, A.C., 1934. On the proportions of organic derivatives in sea water and their relation to the composition of plankton. University Press of Liverpool Liverpool.

Reed, M.H., Strope, E.K., Cremona, F., Myers, J.A., Newell, S.E., McCarthy, M.J., 2023. Effects of filtration timing and pore size on measured nutrient concentrations in environmental water samples. Limnol. Oceanogr. Methods 21, 1–12. https://doi.org/https://doi.org/10.1002/lom3.10529

Reich, T., Belkin, N., Sisma-Ventura, G., Berman-Frank, I., Rahav, E., 2024. Significant dark inorganic carbon fixation in the euphotic zone of an oligotrophic sea. Limnol. Oceanogr. 9999, 1–14. https://doi.org/10.1002/lno.12560

Reich, T., Belkin, N., Sisma-ventura, G., Hauzer, H., Berman-frank, I., Rahav, E., 2026. Does oligotrophy favor chemoautotrophy over photoautotrophy ? Prog. Oceanogr. 241, 103633. https://doi.org/10.1016/j.pocean.2025.103633

Reich, T., Ben-ezra, T., Belkin, N., Tsemel, A., Aharonovich, D., Roth-rosenberg, D., Givati, S., Bialik, M., Herut, B., Berman-frank, I., Frada, M., Krom, M.D., Lehahn, Y., Rahav, E., Sher, D., 2022. A year in the life of the Eastern Mediterranean : Monthly dynamics of phytoplankton and bacterioplankton in an ultra-oligotrophic sea. Deep. Res. Part I 182, 103720. https://doi.org/10.1016/j.dsr.2022.103720

Roshan, S., DeVries, T., 2017. Efficient dissolved organic carbon production and export in the oligotrophic ocean. Nat. Commun. 8, 2036. https://doi.org/10.1038/s41467-017-02227-3

Santinelli, C., 2015. DOC in the Mediterranean Sea, in: Hansell, D.A., Carlson, C.A. (Eds.), Biogeochemistry of Marine Dissolved Organic Matter. Academic Press, London, pp. 579–608. https://doi.org/10.1016/B978-0-12-405940-5.00013-3

Signorini, S.R., Franz, B.A., McClain, C.R., 2015. Chlorophyll variability in the oligotrophic gyres: Mechanisms, seasonality and trends. Front. Mar. Sci. 2, 1–11. https://doi.org/10.3389/fmars.2015.00001

Simon, M., Alldredge, A.L., Azam, F., 1990. Bacterial carbon dynamics on marine snow. Mar. Ecol. Prog. Ser. 65, 205–211.

Simon, M., Azam, F., 1989. Protein-content and protein-synthesis rates of planktonic marine-bacteria. Mar. Ecol. Prog. Ser. 51, 201–213.

Smith, D.C., Azam, F., 1992. A simple, economical method for measuring bacterial protein

754 synthesis rates in seawater using tritiated-leucine. Mar. Microb. Food Webs 6, 107–114.
755 Stanley, R.H.R., Kirkpatrick, J.B., Cassar, N., Barnett, B.A., Bender, M.L., 2010. Net
756 community production and gross primary production rates in the western equatorial
757 Pacific. Global Biogeochem. Cycles 24, GB4001.
758 https://doi.org/https://doi.org/10.1029/2009GB003651
759 Tanioka, T., Garcia, C.A., Larkin, A.A., Garcia, N.S., Fagan, A.J., Martiny, A.C., 2022.
760 Global patterns and predictors of C:N:P in marine ecosystems. Commun. Earth Environ.
761 3, 271. https://doi.org/10.1038/s43247-022-00603-6
762 Teira, E., Serret, P., Fernández, E., 2001. Phytoplankton size-structure, particulate and
763 dissolved organic carbon production and oxygen fluxes through microbial communities
764 in the NW Iberian coastal transition zone. Mar. Ecol. Prog. Ser. 219, 65–83.
765 https://doi.org/10.3354/meps219065
766 Thornton, D.C.O., 2014. Dissolved organic matter (DOM) release by phytoplankton in the
767 contemporary and future ocean. Eur. J. Phycol. 49, 20–46.
768 https://doi.org/10.1080/09670262.2013.875596
769 Torfstein, A., Kienast, S.S., Yarden, B., Rivlin, A., Isaacs, S., Shaked, Y., 2020. Bulk and
770 Export Production Fluxes in the Gulf of Aqaba, Northern Red Sea. ACS Earth Sp.
771 Chem. 4, 1461–1479. https://doi.org/10.1021/acsearthspacechem.0c00079
772 Welschmeyer, N.A., 1994. Fluorometric analysis of chlorophyll a in the presence of
773 chlorophyll b and pheopigments. Limnol. Oceanogr. 39, 1985–1992.
774 Zhang, Y., Huang, Y., Xu, F., Cai, S., Liu, Y., Xu, C., Lin, L., Chen, J., Laws, E.A., Liu, X.,
775 Huang, B., 2025. Decoupling of bacterial production and respiration in the surface water
776 of the North Pacific Subtropical Gyre. Mar. life Sci. Technol. 7, 397–412.
777 https://doi.org/10.1007/s42995-025-00279-9
778 Zohary, T., Herut, B., Krom, M.D., Fauzi C. Mantoura, R., Pitta, P., Psarra, S.,
779 Rassoulzadegan, F., Stambler, N., Tanaka, T., Frede Thingstad, T., Malcolm S.
780 Woodward, E., 2005. P-limited bacteria but N and P co-limited phytoplankton in the
781 Eastern Mediterranean - A microcosm experiment. Deep. Res. Part II Top. Stud.
782 Oceanogr. 52, 3011–3023. https://doi.org/10.1016/j.dsr2.2005.08.011
783